

## **The Influence of Adopting New Reference Breathing Parameters on ICRP66 Model on the Regional Deposition of the Inhaled Attached Radon-222 Daughters Within the Human Airways**

Authors: Belete, Guadie Degu, and Msganaw Shiferaw, Aragaw

Source: Environmental Health Insights, 17(1)

Published By: SAGE Publishing

URL: <https://doi.org/10.1177/11786302221149401>

---

BioOne Complete ([complete.BioOne.org](https://complete.BioOne.org)) is a full-text database of 200 subscribed and open-access titles in the biological, ecological, and environmental sciences published by nonprofit societies, associations, museums, institutions, and presses.


Your use of this PDF, the BioOne Complete website, and all posted and associated content indicates your acceptance of BioOne's Terms of Use, available at [www.bioone.org/terms-of-use](https://www.bioone.org/terms-of-use).

Usage of BioOne Complete content is strictly limited to personal, educational, and non - commercial use. Commercial inquiries or rights and permissions requests should be directed to the individual publisher as copyright holder.

---

BioOne sees sustainable scholarly publishing as an inherently collaborative enterprise connecting authors, nonprofit publishers, academic institutions, research libraries, and research funders in the common goal of maximizing access to critical research.

# The Influence of Adopting New Reference Breathing Parameters on ICRP66 Model on the Regional Deposition of the Inhaled Attached Radon-222 Daughters Within the Human Airways

Environmental Health Insights  
Volume 17: 1–8  
© The Author(s) 2023  
Article reuse guidelines:  
sagepub.com/journals-permissions  
DOI: 10.1177/11786302221149401  


Guadie Degu Belete and Aragaw Msganaw Shiferaw

Department of Physics, College of Natural and Computational Sciences, Assosa University, Assosa, Ethiopia.

**ABSTRACT:** The radiation dose from internal radiation exposure is difficult to measure directly and hence different lung models were developed. The dose on the lung is the result of the regional deposition of aerosols carrying radon daughters in the respiratory tract. Deposition of aerosols can take place during inhalation and exhalation in the 5 regions of the respiratory tract due to variation of aerosol sizes and other biological factors such as breathing rate. In this paper, a modified breathing rate is instead applied on the assumptions developed by the ICRP66 model to analyze the regional deposition of radioactive aerosols and a comparison has been made with the result of ICRP66 model deposition. According to the result, as the diameter of aerosols increases from 1 to 10  $\mu\text{m}$ , the percentage deposition fraction in extrathoracic regions, in ET1 region increases from 6.53% to 48.43% and in ET2 region increases from 7.3% to 50.33%. The aerodynamic deposition of the attached fraction of radon aerosols along the bronchial regions (bronchi (BB), and bronchiolar (bb) region) is found small and almost constant. For 1  $\mu\text{m}$  diameter aerosols, the percentage deposition is found 0.82%, for 5  $\mu\text{m}$  diameter aerosols, the deposition is predicted 2.56% and at 10  $\mu\text{m}$  the deposition is predicted about 1.93% in bronchi (BB) region. In the bronchiolar region (bb) for 1  $\mu\text{m}$  aerosols, the deposition predicted is 1.5% and at 10  $\mu\text{m}$  about 0.88% is predicted. The deposition of small size attached fraction of radon aerosols is found maximum in the alveolar region as compared to other regions of the respiratory tract and the deposition becomes almost negligible for large size aerosols in this region.

**KEYWORDS:** Radon daughters, cancer, activity concentration, bronchial, aerosols, deposition efficiency

**RECEIVED:** July 5, 2022. **ACCEPTED:** December 16, 2022.

**TYPE:** Original Research

**FUNDING:** The author(s) disclosed receipt of the following financial support for the research, authorship, and/or publication of this article: This work is supported by Assosa University ([www.asu.edu.et](http://www.asu.edu.et)).

**DECLARATION OF CONFLICTING INTERESTS:** The author(s) declared no potential conflicts of interest with respect to the research, authorship, and/or publication of this article.

**CORRESPONDING AUTHOR:** Guadie Degu Belete, Department of Physics, College of Natural and Computational Sciences, Assosa University, Assosa 5220, Ethiopia. Email: [guadedegu1@gmail.com](mailto:guadedegu1@gmail.com)

## Introduction

Humans, animals, and plants have been exposed to natural radiation since the creation of life.<sup>1</sup> Radon is major source of background radiation. It contributes about 50% of the natural radiation dose to humans.<sup>2</sup> Radon is a radioactive, colorless, odorless, and tasteless noble gas<sup>3</sup> that can be found in the natural decay chain of uranium isotopes (uranium-238, uranium-236, and uranium-235) in soil, rock, building materials, groundwater, and mining areas and it can be found in the environment surrounding us in varying concentrations. Nevertheless, the ground is the major radon source.<sup>4,5</sup> Since radon-222 is radioactive gas it produces a number of decay products called radon progeny once it has been deposited inside the lung by emitting highly ionizing alpha radiation, beta radiation, or sometimes gamma radiation too.<sup>6,7</sup> When radon-222 daughters are inhaled, a part of them is deposited onto the walls of the respiratory tract. Two of the radon-222 decay products, polonium-218 and polonium-214, emit alpha particles that impart their energies to lung tissues, which is associated with the risk of lung cancer.<sup>8,9</sup>

The decay products of radon (radon-222) are in a solid state and become attached to aerosols and dust particles in the air due to their electrostatic charge. They frequently collide with and attach themselves to large dust particles within the air inside a dwelling. Depending on the concentration of

dust in the room air, up to 80% of the radon decay products will attach to dust particles.<sup>6</sup> The effective size of such attached decay products ranges from 0.05  $\mu\text{m}$  to a few micrometers in diameter.<sup>10</sup> The rate of attachment of radon daughters depends on the following factors: aerosol concentration of the surrounding, the electrostatic charge of the progeny, and humidity of the surrounding environment.<sup>11</sup>

A lot of work has been done to determine the doses in the human lungs due to short-lived radon-222 daughters. Since the dose on lung tissue cannot be measured directly, many lung models were developed to deal with the determination of the dose delivered by alpha particles in the lungs because of their low range and relatively high and discrete energy (6 MeV for <sup>218</sup>Po and 7.69 MeV for <sup>214</sup>Po).<sup>6</sup> ICRP (International Commission on Radiological Protection) model is among those models. ICRP has published 3 different mathematical models to describe the deposition, clearance, and dosimetry of inhaled radioactive materials in the respiratory tract. Because it is based on dividing the respiratory tract into regions, this model is called a deterministic regional compartment model.<sup>12</sup>

In one of the ICRP models, the 1994 version, the respiratory tract is divided into 5 airway regions as shown in Figure 1. The extrathoracic airways are divided into 2 compartments ET1, the anterior nose, and ET2, the posterior nasal passages, larynx, pharynx, and mouth. The bronchial region, (BB,



Creative Commons Non Commercial CC BY-NC: This article is distributed under the terms of the Creative Commons Attribution-NonCommercial 4.0 License (<https://creativecommons.org/licenses/by-nc/4.0/>) which permits non-commercial use, reproduction and distribution of the work without further permission provided the original work is attributed as specified on the SAGE and Open Access pages (<https://us.sagepub.com/en-us/nam/open-access-at-sage>).

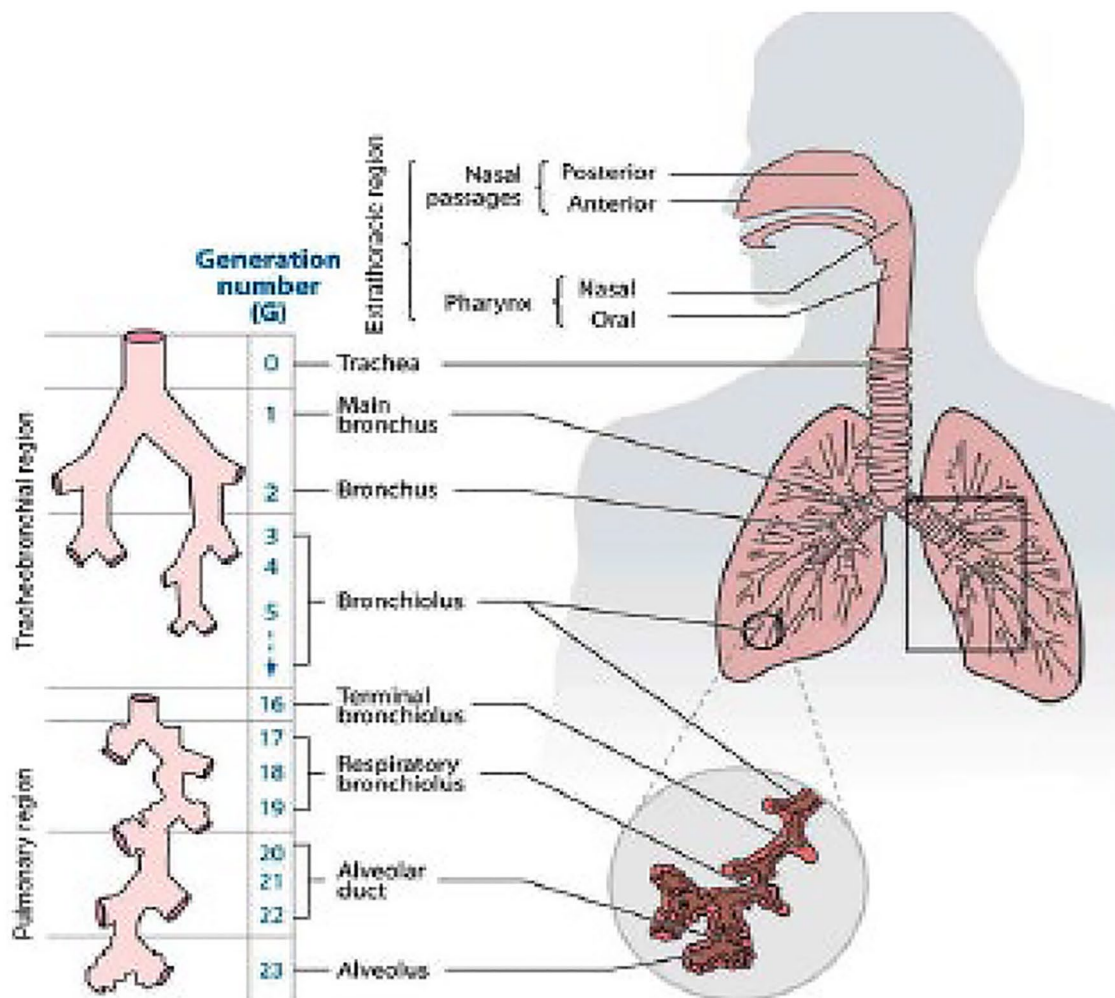


**Figure 1.** Morphological overview of the human respiratory tract.<sup>14</sup>

consists of the trachea, generation 0 and bronchi, from airway generations 1-8), and the bronchiolar region, (bb: from airway generations 9-15), which consists of the bronchioles and terminal bronchioles. The last region is the alveolar-interstitial region AI where gas exchange is performed, consists of the respiratory bronchioles, the alveolar ducts, alveoli, and the interstitial connective tissue.<sup>13</sup>

This study focused on the deposition pattern of aerosols in different regions of an adult's respiratory tract. The deposition model evaluates the fraction of activity in the inhaled air that is deposited in each region. Aerosol deposition in the human respiratory tract is determined by biological factors such as lung morphology, breathing rate, and breathing frequency and physical factors such as fluid dynamics, particle properties, and deposition mechanisms. There are many conditions or parameters that we need to consider in model development. Such as biological factors (breathing rate, breathing frequency, functional residual capacity, tidal volume, volumetric flow rate, target cell depth, thickness of target cell layer, airway dimension, and anatomic dead space) and Physical factors (size of aerosol, density of aerosol, shape factor of aerosol).<sup>13,14</sup>

The deposition of inhaled radon-222 daughters is performed through 3 mechanisms. The first is inertial impaction, in which a droplet fails to turn a corner and impacts the wall of the airway. The second is sedimentation, in which the droplets or particles rain out under the influence of gravity.<sup>15</sup> Finally, there is diffusion caused by Brownian motion, which results in eventual collisions of the droplets with the airway wall.<sup>16</sup> Deposition through impaction or inertial and gravitational sedimentation is more important for the larger particles.<sup>14,17</sup>

### Methodology

For the estimation of regional deposition of the attached fraction of radon-222 daughters, this paper uses a FORTRAN code that runs according to the assumptions of the ICRP model. The computer codes are thus designed to simplify the complicated numerical analysis of deposition fraction in bronchial (BB), bronchiolar (bb), alveolar interstitial (AI), and extrathoracic (ET) regions of the respiratory tract. Regional deposition of the attached fraction of radon depends on biological, physical, and environmental factors. All those exposure conditions should be given to the computer code as input parameters. The values of the input parameters are described

**Table 1.** The values of biological and physical input parameters.

RECOMMENDED PARAMETERS	VALUES ACCORDING TO ICRP
Tidal volume ( $V_T$ )	866.66 mL/ breath
Breathing frequency ( $F_R$ )	15/min
Breathing rate ( $V$ )	0.78 m <sup>3</sup> /h
Functional residual capacity (FRC)	3300 mL
Density ( $\rho$ )	3 g/cm <sup>3</sup>
Shape factor ( $\chi$ )	1.5
Temperature (T)	37°C
Viscosity of air ( $\eta$ )	1.835 × 10 <sup>-5</sup> g/cm.s

by the ICRP committee for a reference of adult Caucasian male 100% nose breather as indicated in Table 1. In this paper a new best estimated breathing rate of 0.78 m<sup>3</sup>/h is used for the deposition analysis of attached fraction of radon-222 daughters and the results of the newly modified breathing parameters on the activity distribution of the inhaled attached radon-222 daughters within the human airways is compared to ICRP66 model deposition.

The anatomic dead space of the regions of the lung affects the regional deposition efficiency of the inhaled activity. Dead space is the volume of inhaled air in each region of the lung that does not participate in the gas exchange process. The dead space in the extrathoracic (ET), bronchi (BB), and bronchiolar (bb) regions is 50, 49, and 47 ml respectively. The diameter of the trachea ( $d_0$ ), bronchi ( $d_9$ ), and terminal bronchiole ( $d_{16}$ ) is also another factor. The regional deposition of aerosols is also depending upon the diameter of airways within the respiratory tract. The aerodynamic and thermodynamic deposition of particulate material in ET1, ET2, BB, bb, and AI regions depends on the values of  $d_0$ ,  $d_9$ , and  $d_{16}$  and their values according to ICRP are 1.65, 0.165, and 0.051 cm respectively. It is the average airway diameter of various airway generations in each region.<sup>18</sup>

If  $C_{in}$  is the amount of radon gas concentration that is diluted with air, the total amount of radon concentration that will be inhaled in a single breath ( $A_{in}$ ) will be the mean value of radon concentration multiplied by tidal volume of the reference person.

$$A_{in} = C_{in} \times V_T \quad (1)$$

The regional deposition fraction of the attached fraction of radon-222 in each region depends on the deposition efficiency of each region. The deposition efficiency of each region is defined as, from the given amount of inhalation how much will be filtered there before passing to the next regions of the respiratory tract. The deposition of large size aerosols (attached

fraction of radon) is expressed in terms of aerodynamic deposition through gravitational settling and inertial impaction. As a result, the deposition efficiency of each region can be found as follow, where  $i$  in each equation represent each region of the respiratory tract.

The deposition efficiency of the extrathoracic ET1 region is given by,<sup>18</sup>

$$\eta_{ET1} = 0.5 \left( 1 - \frac{1}{1 + a_1 R_1^p} \right) \quad (2)$$

The deposition efficiency of the extrathoracic ET2 region is given by,<sup>18</sup>

$$\eta_{ET2} = 1 - \frac{1}{1 + a_2 R_2^p} \quad (3)$$

The deposition efficiency in the bronchi, bronchiolar and alveolar region is given by,<sup>18</sup>

$$\eta_i = 1 - e^{-a_i R_i^p} \quad (4)$$

Following the inhalation of a volume of aerosols, deposition of aerosols takes place in different regions of the respiratory tract which depends on the deposition efficiencies of each region. The deposition efficiency of each region is expressed in the equation above in terms of 3 parameters  $a$ ,  $p$ , and  $R$ . The value of  $a$ ,  $p$ , and  $R$  varies from region to region and also varies during inhalation and exhalation and their values are given in Table 2.  $R$  is breathing rate, transit time, airway diameter, and diameter of the aerosol dependent. Although deposition along each region can take place during the inhalation phase and exhalation phase, the code calculates the deposition during the inhalation phase first, and then it calculates the deposition during the exhalation phase after the gas exchange takes place in alveolar regions. A scaling factor SF is defined as the ratio of a reference airway size in an adult Caucasian male to that in the subject. According to ICRP,<sup>18</sup>  $SF_i$  is 1. Here in Table 2, the aerodynamic diameter  $d_{ae}$  is express in terms of particle diameter  $d_e$ , Cuningham correction  $C(d_e)$ , density  $\rho$  and shape factor  $\chi$  as follows,<sup>18</sup>

$$d_{ae} = d_e \sqrt{\frac{\rho C(d_e)}{\chi \rho_o C(d_{ae})}}$$

Cuningham correction  $C(d_e)$  can be expressed in terms of mean free path and particle size,

$$C(d_e) = 1 + \frac{\lambda}{d_e} [2.514 + 0.8e^{-0.55 \frac{d_e}{\lambda}}]$$

The deposition efficiency of each region depends explicitly on the average transit time of inhaled and exhaled air through each region. The transit times are denoted by  $t_B$ ,  $t_b$ , and  $t_{AI}$ , for the BB, bb, and AI regions, respectively. As transit time between inhaled and exhaled air increased the deposition of aerosols

**Table 2.** Recommended algebraic expressions for aerodynamic deposition.<sup>18</sup>

FILTER	REGION	A	P	R
1	ET1	$3 \times 10^{-4}$	1	$d_{ae}^2 V S F_t^3$
2	ET2	$5.5 \times 10^{-5}$	1.17	$d_{ae}^2 V S F_t^3$
3	BB	$4.08 \times 10^{-6}$ (inhalation) $2.04 \times 10^{-6}$ (exhalation)	1.152	$d_{ae}^2 V S F_t^{2.3}$
4	bb	0.1147	1.173	$(0.056 + t_b^{1.5}) \times d_{ae} t_b^{-0.25}$
5	AI	$0.146 \times S F_A^{0.98}$	0.6495	$d_{ae}^2 t_{AI}$

along each region also increased. The transit time depends on dead space, tidal volume, functional residual capacity, and breathing rate. Transit time in bronchial (BB) and bronchiolar region given by<sup>18</sup>:

$$t_B = \frac{V_D(BB)}{V} \left( 1 + \frac{0.5V_T}{FRC} \right) \quad \text{and} \quad t_b = \frac{V_D(bb)}{V} \left( 1 + \frac{0.5V_T}{FRC} \right)$$

and transit time in the Alveolar Interstitial (AI) region is given by:

$$t_{AI} = V_T - V_D(ET) - (V_D(BB) + V_D(bb))$$

To find the deposition fraction along each region the volumetric fraction of each region must be known. The volumetric fraction is the fraction of the total inhaled volume that will reach in each region of the lung in a single breath. It depends on tidal volume, functional residence capacity, and dead space of the region. Dead space is a little portion or volume of the inspired volume of air that can hold some volume of inhaled air. The air in dead space does not participate in gas exchange. The amount of dead space increases the deposition process. The volumetric fraction of each region is given from equations (5)–(7). It is noted that the volumetric fraction in the extrathoracic region, in ET1 and ET2 is considered nearly one.<sup>18</sup>

$$\psi_{BB} = 1 - \frac{V_D(ET)}{V_T} \quad (5)$$

$$\psi_{bb} = 1 - \frac{V_D(ET) + V_D'(BB)}{V_T} \quad (6)$$

$$\psi_{AI} = 1 - \frac{V_D(ET) + V_D'(BB) + V_D'(bb)}{V_T} \quad (7)$$

Where  $V_D'(BB) = V_D(BB) \left( 1 + \frac{V_T}{FRC} \right)$  and

$$V_D'(bb) = V_D(bb) \left( 1 + \frac{V_T}{FRC} \right)$$

Once the deposition efficiencies  $\eta_i$  and volumetric fraction  $\Psi_i$  of region  $i$  of the respiratory tract are known, the deposition fraction  $D_i$  of region  $i$  can be the product of its deposition efficiency and volumetric fraction.<sup>18</sup>

$$D_i = \eta_i \times \psi_i \quad (8)$$

The computer code uses a do loop that allows variation of diameter of attached fraction aerosols from 1 to 10  $\mu\text{m}$ , and at each diameter the code calculates the deposition efficiencies and percentage of regional deposition. The activity deposited in extrathoracic (ET1) region during inhalation from the total amount of activity inhaled is given as,

$$D_1(ET1) = \eta_{ET1} \times A_{in} \quad (9)$$

The activity after ET1 or brought to ET2 should be total volume of activity that are inhaled  $A_{in}$  minus the activity deposited in ET1,

$$AKT1 = A_{in} - D_1(ET1) \quad (10)$$

All the activity that is brought to ET2 will not deposit on ET2. The activity deposited on ET2 is the product of the deposition efficiency of ET2 and the volumetric fraction that are brought to ET2.

$$D_2(ET2) = \eta_{ET2} \times AKT1 \quad (11)$$

The activity after ET2 or brought to BB should be the total volume of activity that is inhaled  $A_{in}$  minus the activity deposited in ET2 and ET1.

$$AKT2 = A_{in} - D_1(ET1) - D_2(ET2) \quad (12)$$

The activity deposited in BB is,

$$D_2(BB) = \eta_{ET2} \times AKT2 \times \psi_{BB} \quad (13)$$

The activity after BB or brought to bb should be the total volume of activity that is inhaled  $A_{in}$  minus the activity deposited in BB, ET2, and ET1. The activity that is deposited in bb is the product of the deposition efficiency of bb, the volumetric fraction of bb and the volume of activity that is brought to bb. Similar producers are applied to find the deposition on alveolar interstitial (AI) regions. Once the inhaled air reaches the

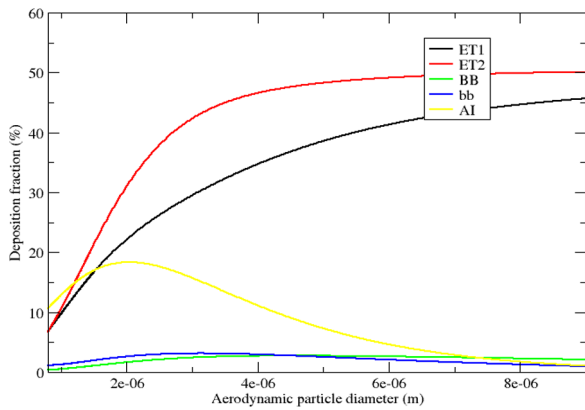


**Figure 2.** Deposition on each region of the respiratory tract.

alveolar regions the gas exchange takes place. The oxygenated blood is transported to parts of the body through pulmonary arteries and the deoxygenated gas will be exhaled. During the exhalation phase of deoxygenated gas from the alveolar region to the external environment, the deposition of aerosols can take place along each region of the respiratory tract.

The activity after AI back to the bronchiolar (bb) region during exhalation is the difference between the activity deposited on each region to the total inhaled air.

$$AKT = A_{in} - \text{Din}(ET1) - \text{Din}(ET2) - \text{Din}(BB) - \text{Din}(bb) - \text{Din}(AI) \quad (14)$$

And hence the amount of activity deposited in bronchiolar (bb) region during exhalation phase can be expressed as,

$$D_{ex}(bb) = \eta_{bb} \times AKT \times \psi_{bb} \quad (15)$$

The code computes the deposition along each region during the exhalation phase. Finally, the total deposition on each region is the sum of the deposition fraction during the inhalation phase plus the deposition fraction during the exhalation phase. The total deposition fraction in the ET1 region can be expressed as,

$$D(ET1) = \frac{D_{in}(ET1) + D_{ex}(ET1)}{A_{in}} \quad (16)$$

In similar way the total deposition fraction of the other regions of the respiratory tract can be determined.

## Results

The deposition of aerosols along the 5 regions of the respiratory tract is studied. The percentage deposition fraction along each region is plotted as the diameter of aerosols increases from 1 to 10  $\mu\text{m}$ .

As shown in Figure 2, as the diameter of aerosols increases from 1 to 10  $\mu\text{m}$ , the percentage deposition fraction in extrathoracic regions, in ET1 region increases from 6.53% to 48.43%, and in the ET2 region increases from 7.3% to 50.33%. The

aerodynamic deposition of the attached fraction of radon-222 aerosols along the bronchial regions (bronchi (BB), and bronchiolar (bb) region) is found small and almost constant as shown in Figure 2. For 1  $\mu\text{m}$  diameter aerosols, the percentage deposition is found 0.82%, around 5  $\mu\text{m}$ , 2.56% and at 9  $\mu\text{m}$  the deposition is predicted about 1.93% in bronchi (BB) region. In the bronchiolar region (bb) for 1  $\mu\text{m}$  aerosols, the deposition predicted is 1.5% and at 9  $\mu\text{m}$  about 0.88% is predicted. As shown in Figure 2 the deposition of the attached fraction of radon aerosols in the alveolar region decreased as the size of aerosols increased, just greater than 2  $\mu\text{m}$ . The deposition of small size attached fraction of radon aerosols is found maximum in this region as compared to other regions of the respiratory tract.

## Discussion

The attached fraction of radon-222 is primarily deposited through an aerodynamic deposition mechanism. The deposition in the upper regions (extrathoracic region) of the respiratory tract is performed through inertial impaction and the deposition in lower regions is using gravitational settling (sedimentation) mechanisms.

As the aerodynamic diameter of the attached fraction of radon-222 aerosols increases as shown in Figure 2, the deposition in the extrathoracic (ET) region becomes larger and larger. This is because during the inhalation, the air speed in the extrathoracic region is high which implies the inertia of attached fractions with larger mass becomes high (product of high mass and also high speed). Moreover, since during inhalation, the airflow undergoes several direction changes in the extrathoracic region, it is difficult for the particles to change directions around the curvatures of the air streams in the extrathoracic regions. Many large particles do not turn with airstream but prefer to travel in the initial directions, and hence they will impact or stick to the surfaces of the turnings and be deposited there through inertial impaction.

As the diameter of aerosols increases from 1 to 10  $\mu\text{m}$ , the deposition fraction in extrathoracic regions, in the ET1 region increases from 6.53% to 48.43%, and in the ET2 region increases from 7.3% to 50.33%. This is due to the fact that as the diameter of the particles increases, their size also increases; in addition to this the speed of the inhaled particles in the extrathoracic region is relatively high which implies the particle's momentum increases. As a result, the particles will be deposited through inertial impaction. For any further increase in the particle size, it is observed that the deposition in the extrathoracic region will be dominant in contrast the deposition in other regions of the respiratory tract becomes negligible.

The nasal hairs in the extrathoracic regions contribute to the filtering process. Most of the large particles are trapped by the nasal hairs which avoids those particles from penetrating into the lung volume. As a result, larger particles will be deposited in the extrathoracic regions.

As shown in Figure 2, the deposition fraction in the alveolar interstitial (AI) region is high for small-size aerosols as compared to other regions of the respiratory tract. The deposition of small size attached fraction of radon-222 is performed through gravitational deposition; they can reach up to the alveolar region as they have small sizes through the inhaled air. But as the size of aerosols increases from 2.38 to 7.11  $\mu\text{m}$ , the deposition process in the alveolar region decreases from 18.3% to 2.75% and becomes almost negligible for large-size aerosols. In the curve, the increase in the total deposition in the alveolar region is shown up to 2  $\mu\text{m}$ , but for the deposition greater than 1  $\mu\text{m}$  diameter, aerodynamic deposition becomes dominant, and hence instead of deposition in the alveolar regions, the deposition in extrathoracic region increases rapidly. And therefore, the deposition of the attached fraction of radon aerosols in the alveolar region gets decreased.

In another way, following the extrathoracic (ET) region, the flow rate (speed) of aerosols in the inhaled air is slightly decreased; this will increase the gravitational settling of the particles. When the speed of air is slow, the residence time becomes longer and hence gravitational sedimentation will take place in the alveolar region. As particle's velocity becomes slower, the particles will have more time to deposit by sedimentation. Gravitational sedimentation becomes more effective in the alveolar region. But as the diameter of the aerosols gets larger and larger, the particles will not have a chance to pass the extrathoracic region. The inertial deposition becomes dominant and the deposition in the alveolar region will approach zero.

The aerodynamic deposition of the attached fraction of radon-222 along the trachea-bronchial regions (bronchi (BB), and bronchiolar (bb) regions) is small and almost constant. There is still deposition of attached fractions through inertial impaction in the bronchi (BB) region as the trachea is divided into left and right bronchi, the inhaled aerosols will be impacted around this branching angle when the airway changes direction. Gravitational settling deposition is performed in the bronchiolar (bb) region as shown in the graph of Figure 2. As particles travel through the air, the gravitational force eventually overcomes their motion, as a result particles will be settled down to the lower surface of the lung (bronchioles (bb)).

Normally, the deposition of the attached fraction of radon-222 is performed through inertial impaction and gravitational sedimentation. The small size part of the attached fraction of radon is deposited through gravitational sedimentation in the alveolar region but as size of the aerosols increases the influence of inertial impaction becomes more effective. Generally, larger particles of the attached fraction of radon aerosols are effectively collected in the extrathoracic region through impaction and small size aerosols are deposited in the alveolar region through gravitational effect, and hence the deposition in the bronchial region does not show any further increase or decrease.

In addition to the effects of particle size and density, the ciliated mucus in the bronchiolar regions contributes to the

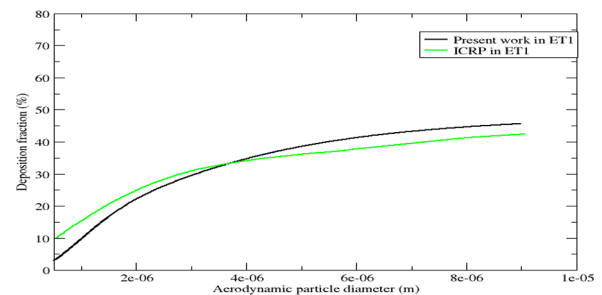


Figure 3. Extrathoracic region (ET1) comparison.

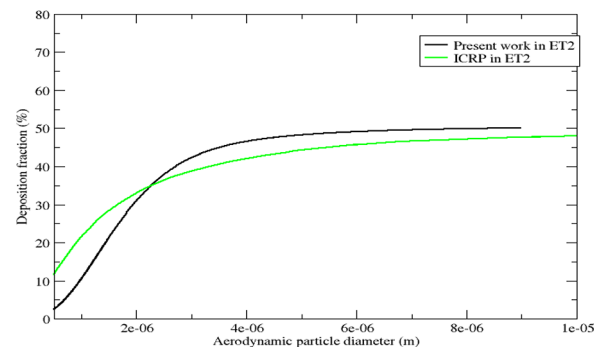


Figure 4. Extrathoracic region (ET2) comparison.

deposition process. As the aerosols flow within the inhaled air in the bronchiolar region, the mucus will capture the incoming aerosols.

Moreover, the deposition of the attached fraction of radon-222 aerosols is dominantly performed in the extrathoracic (ET) region. Their deposition in the lower regions of the respiratory tract (called lung cancer site) is low. The particles which are deposited in the extrathoracic (ET) region can be removed through coughing, sneezing, and swallowing, and hence they will be expelled or ingested. Among the deposited aerosols in the ET2 region, almost all will be cleared by transport to the gastro-inertial (GI) tract in the same way the deposited aerosols in the ET1 region are cleared to the outside environment. Trachea-bronchial region is the main target region for the lung cancer. The decreased deposition in the trachea-bronchial region, however, will lead to a decreased dose supplement to the lung.

### Comparison With ICRP66 Model

The distribution of aerosol deposition in different regions of the respiratory tract for 100% nose adult breather is simulated. The result of the deposition of aerosols in each region of the respiratory tract is compared with the graph developed by the ICRP66 committee. The results of the two plots in each region show a similar deposition pattern with the diameter of aerosols as indicated in Figures 3 to 7.

The deposition in the extrathoracic (ET) region in each plot increases with aerosol size in a similar way the deposition in the alveolar region gets decreased with aerosol size. As shown in Figures 3 and 4, the ICRP66 model predicts slightly larger

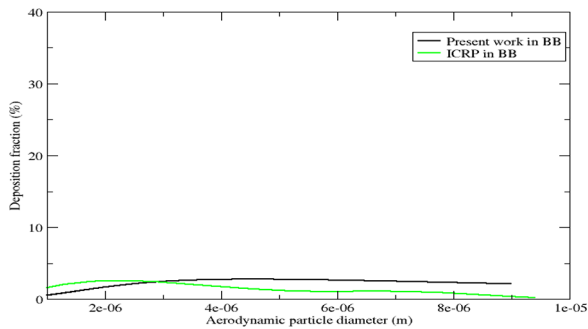


Figure 5. Bronchial (BB) region comparison.

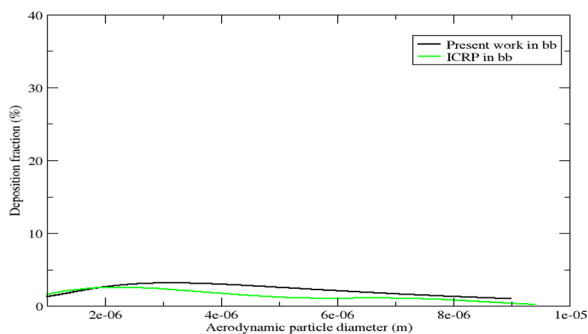


Figure 6. Bronchiolar (bb) region comparison.

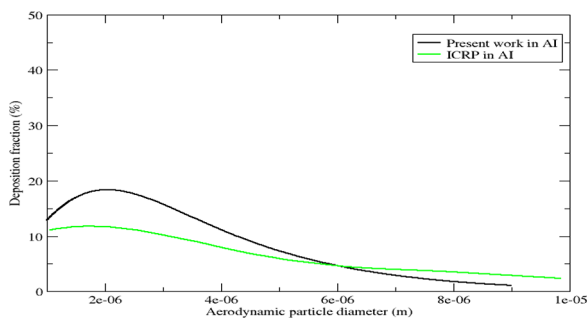


Figure 7. Alveolar (AI) region comparison.

deposition for aerosol diameter in the range from  $1\ \mu\text{m}$  to around  $2\ \mu\text{m}$  in extrathoracic regions.

For a diameter greater than around  $2\ \mu\text{m}$ , the ICRP66 model predicts under estimated deposition fraction. But for the diameter around  $2\ \mu\text{m}$  agreement in deposition fraction is observed between the two plots.

In the bronchial region, an over-estimated deposition fraction is predicted by the ICRP66 model for the aerosol diameter ranging from  $1\ \mu\text{m}$  to around  $2\ \mu\text{m}$  as compared to the present work as shown in Figure 5. The two predictions agree on the diameter approximately  $2\ \mu\text{m}$ . In alveolar regions for aerosol diameter between  $1\ \mu\text{m}$  to around  $6\ \mu\text{m}$ , the present work predicts under estimated deposition fraction whereas for a diameter greater than  $6\ \mu\text{m}$  the ICRP66 model predicts a slightly larger deposition fraction as shown in Figure 6.

This little discrepancy between the present work and ICRP66 mode is due to a modification of parameters. The data for ICRP 66 plots in each region above is generated by extracting the regional deposition plot of the ICRP 66

publication which is based on a breathing rate of  $1.2\ \text{m}^3/\text{h}$  (sitting and light exercise). But the simulated graph (the black one) along each region is plotted at a flow rate of  $0.78\ \text{m}^3/\text{h}$ . The two deposition plots were compared to see the deposition deviation. The other parameters were kept constant in both cases. This is because in our simulation the best estimated newly modified ICRP parameter values are used, to fit with the experimental measurements.

## Conclusions

The radioactive radon-222 and its decay products can attach to the solid dust particles or aerosols in the air and hence can be easily inhaled. Many lung models were developed to study the deposition of aerosols in the respiratory system. In this work, a comparison of a deposition estimated by modified breathing rate parameter and ICRP66 model deposition was performed. The resulting deposition from the modified breathing rate aerosols in the extrathoracic, bronchial and alveolar region were compared with the deposition predicted by ICRP66. According to the comparison, the deposition predicted by modified parameter is slightly different from ICRP 66 deposition prediction. The result of this paper showed that most of the deposition of attached fraction of radon-222 daughters is performed in extrathoracic region compared to the lower regions of the respiratory tract and hence one can conclude that the attached fraction of radon-222 daughters have less contribution to induce lung cancer.

## Acknowledgement

The authors would like to express sincere gratitude to Assosa University for providing the necessary financial and material support during the thesis work of this study.

## Author Contributions

The authors confirm contribution to the paper as follows: study conception, design, simulation, analysis and interpretation of results: Guadie Degu Belete; editing the draft manuscript and organizing the structure: Aragaw Msganaw Shiferaw. All authors reviewed the results and approved the final version of the manuscript.

## REFERENCES

1. Ravikumar P, Somashekar RK. Estimates of the dose of radon and its progeny inhaled inside buildings. *Eur J Environ Sci*. 2013;3:88-95.
2. Shahbazi-Gahrouei D, Gholami M, Setayandeh S. A review on natural background radiation. *Adv Biomed Res*. 2013;2:65.
3. Pawel DJ, Puskin JS. The US environmental protection agency's assessment of risks from indoor radon. *Health Phys*. 2004;87:68-74.
4. Bowie C, Bowie SH. Radon and health. *Lancet*. 1991;337:409-413.
5. Degu Belete G, Alemu Anteneh Y. General overview of radon studies in health hazard perspectives. *J Oncol*. 2021;2021:6659795.
6. Mohamed A, Ahmed AA, Ali AE, Yuness M. Attached and unattached activity size distribution of short-lived radon progeny (214pb) and evaluation of deposition fraction. *J Nucl Radiat Phys*. 2008;3:101-108.
7. Papenfuß F, Maier A, Fournier C, Kraft G, Friedrich T. In-vivo dose determination in a human after radon exposure: proof of principle. *Radiat Environ Biophys*. 2022;61:279-292.
8. Chalmers B, Mangiaterra V, Porter R. WHO principles of perinatal care: the essential antenatal, perinatal, and postpartum care course. *Birth*. 2001; 28:202-207.



9. Cousins C, Miller DL, Bernardi G, et al.; International Commission on Radiological Protection. ICRP PUBLICATION 120: radiological protection in cardiology. *Ann ICRP*. 2013;42:1-125.
10. Chamberlain AC. *Radioactive Aerosols*. Vol. 3. Cambridge University Press; 2004.
11. Sakoda A, Ishimori Y, Fukao K, Yamaoka K, Kataoka T, Mitsunobu F. Lung dosimetry of inhaled radon progeny in mice. *Radiat Environ Biophys*. 2012;51:425-442.
12. Hofmann W. Overview of radon lung dosimetry. *Radiat Prot Dosimetry*. 1998;79:229-236.
13. Winkler-Heil R, Hofmann W, Marsh J, Birchall A. Comparison of radon lung dosimetry models for the estimation of dose uncertainties. *Radiat Prot Dosimetry*. 2007;127:27-30.
14. Hussain M, Madl P, Khan A. Lung deposition predictions of airborne particles and the emergence of contemporary diseases, Part-I. *Health*. 2011;2:51-59.
15. Hofmann W. Modelling inhaled particle deposition in the human lung—a review. *J Aerosol Sci*. 2011;42:693-724.
16. Carvalho TC, Peters JI, Williams RO 3rd. Influence of particle size on regional lung deposition—what evidence is there? *Int J Pharm*. 2011;406:1-10.
17. Heyder J. Deposition of inhaled particles in the human respiratory tract and consequences for regional targeting in respiratory drug delivery. *Proc Am Thorac Soc*. 2004;1:315-320.
18. ICRP. Human respiratory tract model for radiological protection: ICRP publication no. 66. *Ann ICRP*. 1994;27:1-3.